Sea level variability in the Mediterranean Sea through satellite altimetry analytical covariance functions

D.A. Natsiopoulos, G.S. Vergos, I.N. Tziavos, V.N. Grigoriadis

Aristotle University of Thessaloniki, Department of Geodesy and Surveying, Thessaloniki, GR-54124, Greece

Abstract: Since the early 80's satellite altimetry resulted in an abundance of sea surface height measurements. These data are crucial to both oceanographic and geodetic applications while the realization of the recent gravity-field dedicated missions of GRACE and GOCE offer gradiometric and range-rate data about the Earth's gravity field. The proper combination of these heterogeneous data offer new opportunities for the estimation of sea level and dynamic ocean topography trends. In related studies, even though the data combination and processing strategies have been carried out carefully with proper control, error propagation through analytical data variance-covariance matrices has been given little attention. The latter is of great importance since it can provide reliable estimates of the output signal error. The optimal operator for such purposes, widely used in physical geodesy, is Least Squares Collocation (LSC), which needs the input data and error variance-covariance matrices to be known. The latter are traditionally derived from the analytical covariance functions of the input signals, a.k.a., Sea Level Anomalies (SLA) in the case of altimetry. This work presents results on the determination of analytical covariance functions for the SLA in the Mediterranean Sea as well as an analysis of the SLA variability in this semi-enclosed marine region. The raw data used are SLAs from ENVISAT for the entire duration of the satellite mission (2002-2011), employed to derive linear trends about the SLA variation in the area under study and come to some conclusions on the Mediterranean variability at short scales. Then, SLA analytical covariance functions are estimated based on 2nd and 3rd order Gauss-Markov models and exponential ones. Conclusions are drawn based on prediction errors with LSC, while evidence of the cyclo-stationarity of the SLA is deduced.

Keywords: cyclo-stationarity, Gauss-Markov models, least-squares collocation, sea level anomalies, sea variability.

1. Introduction

The global average level of the Earth's oceans and its variation over various time and spatial scales is one of the most important indicators of climate change (*AVISO, 2013*). Sea level has a rising trend and coastal erosion, inundation of land, increased flood, storm damage, increased salinity of estuaries and aquifers are some indicators of this trend. Many factors that take place within system Earth af-

fect sea level change at various scales. Some of them are not directly climate related, like tides, storm surges or atmospheric effects while others like isostatic, steric and eustatic effects are directly related to climate change. Natural processes in the physical properties of the ocean water and water mass transport between the Earth's oceans, continents and the atmosphere result in steric sea level changes. Variations in the seawater density triggered by salinity and temperature changes result in the former sea level changes. Ocean warming results to density decrease and even at constant mass, the volume of the ocean increases. Thermal expansion occurs at all ocean temperatures so that with higher temperature water expands more. Consequently, the averaged thermal expansion at a global scale is correlated with the distribution of heat within the seas (*Bindoff et al., 2007*). On the other hand, variations in the water salinity have a direct impact on the variations of the local water density and sea level, but do not influence global average estimates, since local effects are canceled out in global estimations. On the other hand, volumetric changes trigger the eustatic (non-steric) changes. Water mass transport due to changes in the continental reservoirs (river run-off), glacial and ice caps mass variations (melting) and atmospheric water vapor changes (precipitation and evaporation) affect volumetric changes (*Chen et al., 2005; Chambers et al., 2004; Garcia et al., 2007*).

The proper modeling of Sea Level Anomaly (SLA) variations is essential when data combination and error propagation are used to determine the Dynamic Ocean Topography (DOT) or to model the marine geoid *Knudsen (1993*). With the advent of the recent gravity-field dedicated missions of GRACE and GOCE, an abundance of gravity data for the oceans became available, allowing the combined use of gravity field parameters with satellite altimetry observations to study the Earth's oceans (*Barzaghi et al., 2009; Vergos et al., 2012*). The optimal operator for such purpose used in physical geodesy is least-squares collocation (LSC), which needs the input data and error variance-covariance matrices to be known.

Monitoring of the sea level has been traditionally carried out with tide-gauge stations located in coastal areas around the globe. This situation arrived at a landmark on the early 80's when altimeters on-board satellites resulted in the availability of sea surface height measurements with global coverage, homogeneous accuracy and unprecedented resolution. This abundance of measurements for the Earth's oceans leads to an improved knowledge of the monitoring of sea level variations over large time and spatial scales. The realization of the GRACE and GOCE missions offers new opportunities for the estimation of sea level variations with heterogeneous data combination (*Tziavos et al., 2013*). In such studies, the full variance-covariance matrices are needed for the input data since rigorous modeling of the signal and error characteristics is essential. When the aim is the determination of SLAs or the DOT from heterogeneous data, one can determine analytical covariance functions for the disturbing potential, its derivatives and geoid heights using

available a-priori information (*Vergos et al., 2012; 2013*). However, analytical models for altimetric SLAs are not available, so that their proper modeling and determination is crucial for combination studies. The focus of this work is on the proper modeling of available SLA data in order to determine empirical and analytical covariance functions, so that they will subsequently be used for prediction with LSC. From the available analytical covariance functions the full variance-covariance matrices of the functional under study, i.e., the SLA or the DOT can be derived. The raw data used are SLA values from ENVISAT satellite for the entire duration of the satellite mission (2002-2011). Both along-track (1D) and cross-track (2D) cases are studied interpreting the empirical and modeled characteristics of the covariance functions. Along-track records of the SLA have been used both to derive linear trends of the SLA variation in the area under study and come to some conclusions on the Mediterranean variability at short scales. The estimation of the analytical covariance functions is performed using 2nd and 3rd order Gauss-Markov models and exponential models, which are then used for prediction with LSC. Conclusions based on prediction errors with LSC are drawn so that the most proper analytical model can be determined. Finally, the so-derived SLA variances are used to investigate the possible cyclo-stationarity of the SLA.

2. Available data, area under study and PRe-Processing

The area under study spans the entire Mediterranean Sea bounded between $30^o \leq \varphi \leq 50^o$ and $-10^o \leq \lambda \leq 40^o$. In this region, the statistical characteristics of the SLA have been studied using altimetric observations from ENVISAT for the entire duration of its mission (2002-2011). The ENVISAT data where acquired from the RADS system (*RADS*, 2012) which has a collection of data of past and current satellite altimetry missions. The altimetric data were available in the form of SLAs referenced to a *"mean-sea*-surface*"* that depends on user selection within the RADS system. Therefore*,* it was decided to refer the data to the EGM2008 geoid *Pavlis et al. (2008*), keeping in mind that a zero-tide (ZT) geoid model is adopted to be in-line with the tide-conventions used in altimetric data processing. All geophysical and instrumental corrections have been applied, using the default models proposed by the RADS system. Those were a) ECMWF for the dry tropospheric correction, b) MWR(NN) for the wet tropospheric correction, c) the smoothed dual-frequency model for the ionospheric correction, d) tidal effects due to Solid Earth, Ocean, Load and Pole from the Solid Earth tide, GOT4.7 ocean tide, GOT4.7 load tide and pole tide models respectively, and e) the CLS Sea State Bias (SSB) model for the SSB effect *Naeije et al. (2008*). The mesh of values is dense enough and it is composed by ~1003 passes, with a cross-track spacing of 75 km at the equator. As far as the Inverse Barometer (IB) correction is concerned, this has not been applied because the total inverse barometer correction has little effect to

the “global” SLA statistics. In order to create a database with solely sea level data, all values located close to coastal areas and islands, or affected by various instrumental errors, have been removed.

The first part of this work refers to the identification of sea level variations within the satellite repeat period, i.e., for periods as short as 35 days for ENVISAT. In order to investigate such variations, a single pass was selected from ENVISAT based on the following criteria: a) the pass shall be long and span the entire basin in the north-south or south-north direction (ascending or descending pass respectively), b) there shall be no or little land intrusion from isles or islands in the SLA records of the pass, c) the data record shall be as consistent as possible throughout the satellite data record for the period of study, i.e., missing records and/or voids should be kept to a minimum. Based on these criteria, it was decided that ENVISAT pass 399 would be studied. ENVISAT pass 399 is a descending one crossing the entire eastern Aegean Sea, starting in the North off the coast of Thasos, crossing Lemnos, then eastern Cyclades, and finally after crossing the strait between Crete and Karpathos enters the Libyan Sea and ends near the coasts of Egypt (see Figure 1).

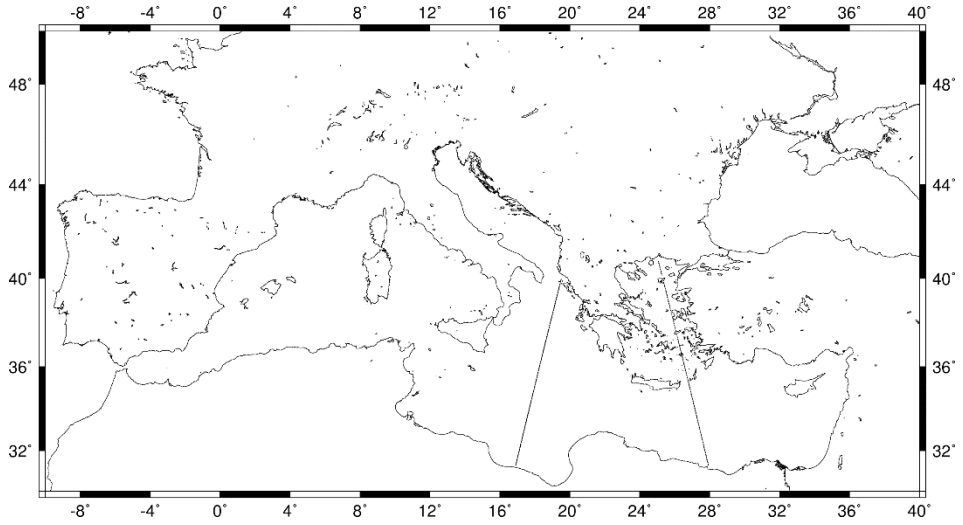

Figure 1: *ENVISAT pass 399 (descending through the Aegean Sea) and pass 444 (ascending through the Ionian Sea).*

In the second part of this work, the estimation of SLA analytical covariance functions based on two main sets of tests has been carried out. The first one refers to the use of a single pass of the satellite, in order to study the stochastic characteristics of the SLA in the along-track (1D) direction. For that case, the longest pass available in the Mediterranean Sea (pass 444) has been used in order to utilize as many as possible SLA observations without any interruptions from dry-land areas (islands,

isles, etc.). ENVISAT pass 444 is an ascending one, starting from northern Libya, crossing the central part of the Mediterranean Sea, passing east of Malta and ends off the coasts of Corfu (see Figure 1). The second test refers to the use of the entire set of ENVISAT passes for the Mediterranean Sea so that the SLA variability will be studied in both the along- and cross-track (2D) direction (see Figure 2).

3. SLA empirical and analytical covariance functions for prediction with LSC

As already mentioned the statistical characteristics of the SLA will be studied using observations from ENVISAT employing a stochastic approach. Within this frame, first the empirical covariance functions for each 35-day repeat period are determined for the entire satellite missions. Then, the so-derived statistical characteristics are used to analyze the SLA variability on one hand and determine analytical covariance function models on the other. The latter are then employed for SLA prediction with LSC where two main sets of tests have been carried out. The first one refers to the use of a single pass of the satellite, so as to study the stochastic characteristics of the SLA in the along-track (1D) direction (pass 444) while the second one refers to the use of the entire set of ENVISAT passes for the Mediterranean Sea so that the SLA variability will be studied in both the along (1D) and cross-track direction (2D).

In order to represent the local statistical characteristics of the signal under consideration, first the empirical covariance models must be derived. Assuming that the observations are given in discrete points in the area, the calculation of the covari-

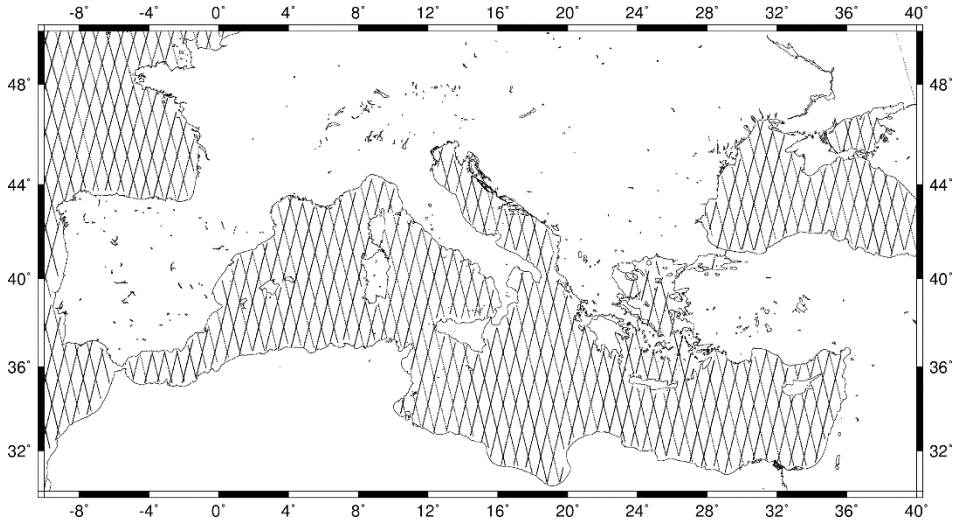

Figure 2: *ENVISAT data distribution in the Mediterranean Sea.*

ance function is then done by numerical integration (*Tcherning and Rapp 1974)*. If each observation y_i represents a small area A_i and y_j represents an area A_j then the empirical covariance is:

$$C_k = \frac{\sum A_i A_j y_i y_j}{\sum A_i A_j}, \tag{1}$$

where, ψ is the spherical distance and

$$\psi_{k-1} < \psi_{ij} < \psi_k . \tag{2}$$

If the area is subdivided into small cells holding one observation each and A_i and A_j are assumed to be equal then Eq. (1) reduces to

$$C_k = \frac{\sum y_i y_j}{N_k}, \tag{3}$$

where, N_k is the number of products $y_i y_j$ in the k^{th} interval (*Knudsen 1987)*. In our case the empirical covariances of SLA (h^{SLA}) for a given spherical distance ψ is:

$$C\left(h_i^{SLA}, h_j^{SLA}, \psi\right) = M\left\{h_i^{SLA} h_j^{SLA}\right\}_\psi . \tag{4}$$

In order to determine some analytical model for the SLA covariance function, various options have been tested. In all cases the analytical covariance function models should agree to the empirical values available for the area under study in order to represent the local statistical characteristics of the signal under consideration. For the 1D case, the empirical covariance function for pass 444 has been estimated for the entire duration of the mission. The first class of analytical models refers to exponential ones, the second refers to 2nd and 3rd order Gauss-Markov, while an analytical model similar to the one used by *Tscherning, and Rapp (1974)* for the disturbing potential has been tested. For the exponential models six choices were examined, with varying number of parameters to be determined as follows:

$$C_{h^{SLA}h^{SLA}}(\psi) = \alpha e^{b\psi}, \tag{5}$$

$$C_{h^{SLA}h^{SLA}}(\psi) = \alpha e^{b\psi} + c e^{d\psi}, \tag{6}$$

$$C_{h^{SLA}h^{SLA}}(\psi) = \alpha e^{-\left(\frac{\psi - b}{c}\right)^2}, \tag{7}$$

$$C_{h^{SLA}h^{SLA}}(\psi) = \alpha e^{-b\psi^2}, \tag{8}$$

$$C_{h^{SLA}h^{SLA}}(\psi) = \alpha e^{-b\psi} \cos(\omega\psi), \tag{9}$$

$$C_{h^{SLA}h^{SLA}}(\psi) = \alpha(1 + b\psi) e^{-b\psi} . \tag{10}$$

In Eqs. (5)-(10), *a*, *b*, *c* and *d* denote parameters to be determined, so that the analytical covariance model will fit the empirical one. The 2nd and 3rd order Gauss-Markov models are outlined in Eqs. (11) and (12) respectively, where *D* is the characteristic distance, *r* is the planar distance and $\sigma^2_{h^{SLA}}$ the SLA variance *(Jordan, 1972; Knudsen and Tscherning 2007):*

$$C_{h^{SLA}h^{SLA}}(r) = \sigma^2_{h^{SLA}}\left(1+\frac{r}{D}\right)e^{\left(-r/D\right)}, \tag{11}$$

$$C_{h^{SLA}h^{SLA}}(r) = \sigma^2_{h^{SLA}}\left(1+\frac{r}{D}+\frac{r^2}{3D^2}\right)e^{\left(-r/D\right)}. \tag{12}$$

Finally, the last model that has been tested was:

$$C_{h^{SLA}h^{SLA}}(\psi) = \sum_{n=0}^{\infty}\sigma_n^2\left(h^{SLA}\right)P_n\left(cos\,\psi\right), \tag{13}$$

where, $\sigma_n^2\left(h^{SLA}\right)$ are the degree variances of the SLA and $P_n(cos\psi)$ denotes the Legendre polynomials. For the description of the behavior of the degree variances given in Eq. (13) a 3rd degree Butterworth filter is used so that the degree variances of the SLA are given as (*Knudsen and Tscherning, 2007*)

$$\sigma_n^2\left(h^{SLA}\right) = b\left(\frac{k_2^3}{k_2^3+n^3}+\frac{k_1^3}{k_1^3+n^3}\right)s^{n+1}. \tag{14}$$

The factors *b*, k_1, k_2 and *s* are estimated by least-squares, so that the analytic model fits the empirical values describing the statistical characteristics of the functional in the area under study and more precisely the variance and the correlation length. Note that the scale factor s^{n+1} in Eq. (14) resembles the $(R_B/R)^{2(n+1)}$ term in the Tscherning and Rapp analytical covariance model of the anomalous potential. Given the analytical expressions for the covariance functions of the SLA observations, it is possible to proceed to the simultaneous estimation of the output signals along with their prediction errors. In the present work, the prediction with LSC will be carried out in both the along track direction (1D case) and Mediterranean-wide (2D case), where the SLA signal to be predicted will be omitted from the input data, so as to determine the estimation accuracy. In this case, both the available observations and the signal to be predicted are SLAs, so that the estimation is carried out as (*Knudsen and Tscherning, 2007; Tscherning and Rapp, 1974*):

$$\hat{h}^{SLA}(P) = \boldsymbol{C}_{\hat{h}^{SLA}h^{SLA}}(P,\cdot)\boldsymbol{C}^{-1}_{h^{SLA}h^{SLA}}\boldsymbol{h}^{SLA}. \tag{15}$$

In Eq. (15), $\hat{h}^{SLA}(P)$ denotes the SLA to be predicted at point *P*, $\boldsymbol{h}^{SLA}$ is the vector of observations, $\boldsymbol{C}_{\hat{h}^{SLA}h^{SLA}}(P,\cdot)$ is the cross-covariance matrix between the SLA to be

predicted and the input signals and $\boldsymbol{C}_{h^{SLA}h^{SLA}}$ is the full variance-covariance matrix of the input SLAs determined from the analytical covariance function model used.

4. SLA variations in the mediterranean Sea

4.1 SLA variations from the along-track ENVISAT records

As already mentioned, the first part of this work refers to the identification of sea level variations within the satellite repeat period for periods as short as 35 days. Table 1 summarizes the statistics of the annual ENVISAT SLAs (cycles 6 to 94), for the entire Mediterranean Sea, after the application of all geophysical corrections except that of the global and local IB ones. From that Table a variation of the order of ~3.3 cm can be seen in terms of the std, while the large discrepancies in the minimum and maximum values can be attributed to blunders located in all cases close to the coastline. Before proceeding any further to the utilization of the SLA data for MSL or sea level variations studies, a 3σ test has been applied in order to remove blunders. It should be noted that in order to apply such a blunder detection and removal test, the data are regarded as bias free, which for the case of the ENVISAT observations holds since the mean value of the former is at the 3 cm level. Such small mean values can be safely regarded as close to zero, so that the data can be treated as bias free. A total number of 679k observations from ENVISAT were available, out of which only 8502 (1.2%) have been identified as blunders and removed. Table 1 summarizes the statistics of the ENVISAT SLA record before and after the 3rms test.

Table 1: *Statistics of annual ENVISAT (phase B) SLAs and global statistics before and after the blunder detection and removal. Unit: [m].*

Year	period	cycles	min	max	mean	std
2002	14-5-02 to 13-1-03	6-12	-0.552	1.044	0.073	±0.134
2003	13-1-03 to 2-2-04	13-23	-0.773	1.015	0.007	±0.140
2004	2-2-04 to 17-1-05	24-33	-0.802	1.061	0.025	±0.156
2005	17-1-05 to 2-1-06	34-43	-1.142	1.179	0.029	±0.153
2006	2-1-06 to 22-1-07	44-54	-1.391	0.893	0.036	±0.146
2007	22-1-07 to 7-1-08	55-64	-2.781	0.805	0.030	±0.128
2008	7-1-08 to 24-1-09	65-75	-0.727	0.798	0.026	±0.136
2009	26-1-09 to 11-1-10	76-85	-0.761	0.725	0.046	±0.136
2010	11-1-10 to 22-10-10	86-94	-0.523	0.897	0.056	±0.167
Before blunder removal			-2.781	1.179	0.028	±0.143
After blunder removal			-0.433	0.433	0.022	±0.133

With the so-derived *"blunder-free"* SLAs, an analysis of the SLAs for pass 399 was carried out on a per-cycle basis. Each time, the available SLAs for the same pass and three consecutive cycles were analyzed, so that more than three months are covered (e.g., cycle 23 is analyzed together with cycles 24 and 25 so that a total of ~105 days is studied). Moreover, the SLA residuals between the studied cycles, i.e., the differences between the available SLAs for the three consecutive cycles were determined as well. It should be noted that the analysis presented herein will refer to 2003 onwards, since the first ENVISAT cycles (6-12) had few records available due to the problems with the satellite microwave radiometer. From the analysis of the first repeated ENVISAT cycles 23-24-25 a variation of the order of ~10 cm was evidenced, while if this bias was neglected then the SLA records followed the same periodic pattern of decreased and increased sea level with increasing latitude. Therefore, it is expected that a trend within these three cycles would not be evident. This was confirmed by inspecting the SLA differences between cycles 23, 24 and 25, since the estimated trends were between +4 mm/35-days and -2 mm/35-days. From the analysis of the respective SLAs for cycles 33, 34 and 35, it was interesting to notice that cycle 34 missed a significant number of records compared to the others (64 sub-satellite observations compared to 130 ones for cycles 35 and 36). Moreover, cycle 34 follows closely the other two cycles analyzed until $\varphi=34.3^o$ (approximately at the south-east corner of Crete), and as the satellite moves to northern latitudes it deviates significantly with a bias of the order of ~15-20 cm. This is a good indication that the available SLA records from that cycle contains blunders, since when investigating the mean wind-speed for each cycle it was found that they do not deviate significantly (the wind speed ranges between 6.6 m/s, 10.7 m/s and 7.2 m/s for cycles 33, 34 and 35 respectively). Therefore, wind-drives SLA variations that were not treated by the applied IB correction cannot be blamed for the deviations found. When investigating the differences between the three cycles it is found that a positive trend of +6 mm/35-days exists between cycles 34 and 35, while a negative trend of –5 mm/35-days exists between cycles 33 and 34. As a consequence, no trend is found in the 3-month period covered by cycles 33 and 35. Analyzing the SLA records for cycles 44, 45 and 46 covering the first three months of 2006, an interesting agreement is found between the consecutive records of the satellite. By inspecting their records, almost no bias exists between the SLAs since this is at the 5 cm level at most. Once again, one cycle misses a significant number of records, that is cycle 46, since no SLA data are available north of $\varphi=39.6^o$. Nevertheless, the same problems as with cycle 34 are not evidenced for the rest of the cycle records, since they do not present any extreme, blunder-like, variations compared to cycles 44 and 45. From that analysis of the differences between the SLAs, a zero trend is found between cycles 44 and 45, while the sea rises by +2 mm/35-days between cycles 45 and 46, and the same trend holds between cycles 44 and 46 as well. Similar results are found for 2008, i.e., cycles 64, 65 and 66 where a positive trend of +2.1 mm/35-days is found,

which increases to +4 mm/35-days for 2009, cycles 74, 75 and 76 and reduces to +1 mm/35-days for 2010, cycles 84, 85 and 86.

4.2 SLA empirical covariance functions and variability

Following Eq. 4, the empirical covariance functions for pass 444 have been estimated for all available ENVISAT cycles. Given the 35-day repeat period of ENVISAT, it is implied that for each year ~11 covariance functions have been determined, using a spherical distance ψ class size equal to 15 km. Some examples for pass 444 are presented in Figure 3 below, where the empirical covariance functions for 2005 and 2009 are depicted. From the empirical covariance function for 2005 it is interesting to notice the changes in variance during the entire year. The variance varies from 74 cm^2 in January to ~30 cm^2 in February, March and April, then to 67 cm^2 in May, 52 cm^2 in June, climax to ~100 cm^2 for August, September and October and then fall again to ~70 cm^2 for November and December. This variation follows the thermal expansion of the sea, due to the increasing temperatures during the summer and early fall months and the lower temperatures during winter. Moreover, the seasonal cycle can be also attributed to atmospheric forcing due to the variation in atmospheric pressure in the Mediterranean. The latter can be investigated in connection with well-known climate indices like SOI, NAO and MOI. By studying the year 2008, it is observed that the variance for the winter months is much lower than the summer ones, e.g., the variance is at ~23 cm^2 in January, then rises to ~85 cm^2 in July and reaches ~110 cm^2 in August, to drop again to nominal values for fall and winter. This significant variation in the variance for the winter months in 2008 can be attributed to the influence of some climatic forcing of the Mediterranean SLA. Given that the empirical covariance functions for pass 444 will be used for the along-track prediction with LSC in the following section, the same procedure has been followed for the determination of the empirical covariance functions for the 2D case. As far as the 2D case is concerned, two options have been tested in order to estimate SLAs with LSC after determining analytical covariance function models. First, empirical covariance functions have been estimated using a complete cycle of the ENVISAT data for the entire Mediterranean Sea (all passes included, see Figure 3). In this option, cycle 74 with a total number of 11870 SLA observations is used. The second test refers to a window data for the area bounded between $32^o \leq \varphi \leq 36^o$ and $15^o \leq \lambda \leq 20^o$. The step for the spherical distance ψ is set to 15 km in these two cases, and the covariance functions determined are presented in section 5.

Before that step, it is interesting to see the variability of the SLA variances through time and investigate whether time-dependent patterns can be determined. Figure 4 depicts the variation of the SLA signal variance with time between 2005 and 2010, where 4-month (dash-dot line) and a 6-month (long-dashed line) moving averages have been plotted to outline semi-annual and seasonal variations. It should be noted

that the years spanning from 2002-2004 have not been included in this analysis due to the reduced number of SLA observations, so as not to bias any conclusions drawn. From Figure 4 it is evident that there is an annual and seasonal pattern in the ENVISAT SLA variances, with the largest values occurring in the summer months (June-July-August of each year) and the smallest ones in the fall. This is more evident in the years 2008 and 2009, where the smallest and largest amplitude values of the SLA spectra can be seen (January and August 2008 respectively). Moreover, a significant positive trend is also evident starting from the low in May 2008 and propagating to the high amplitude in August of the same year, which is correlated with climate forcing in the SLA as will be shown in the sequel. In any case, given that the SLA variation for the particular pass shows a clear cyclo-stationarity at least on an annual basis, the analysis has been extended to other ENVISAT passes in the Mediterranean Sea. From that it was concluded that basin-wide the Mediterranean SLA variability shows cyclo-stationarity, even though not homogeneous since the rise during the summer months is more evident in the south-east part (Levantine Sea).

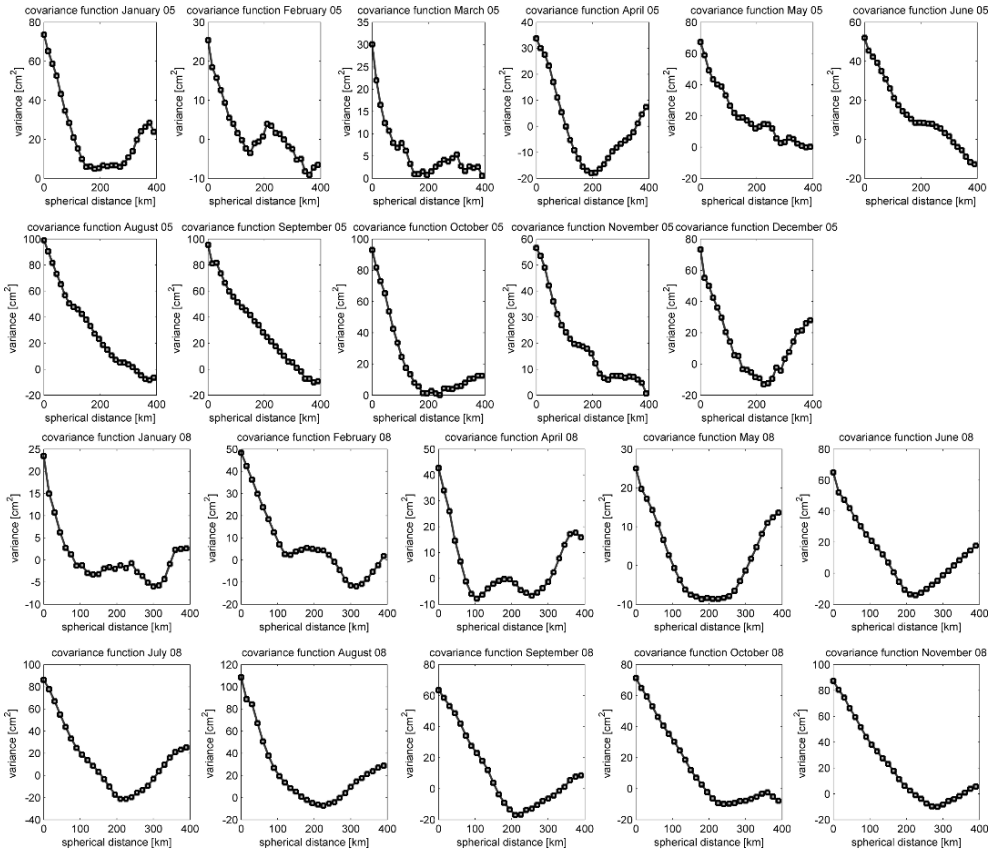

Figure 3: *ENVISAT pass 444 empirical covariance functions for years 2005 and 2008.*

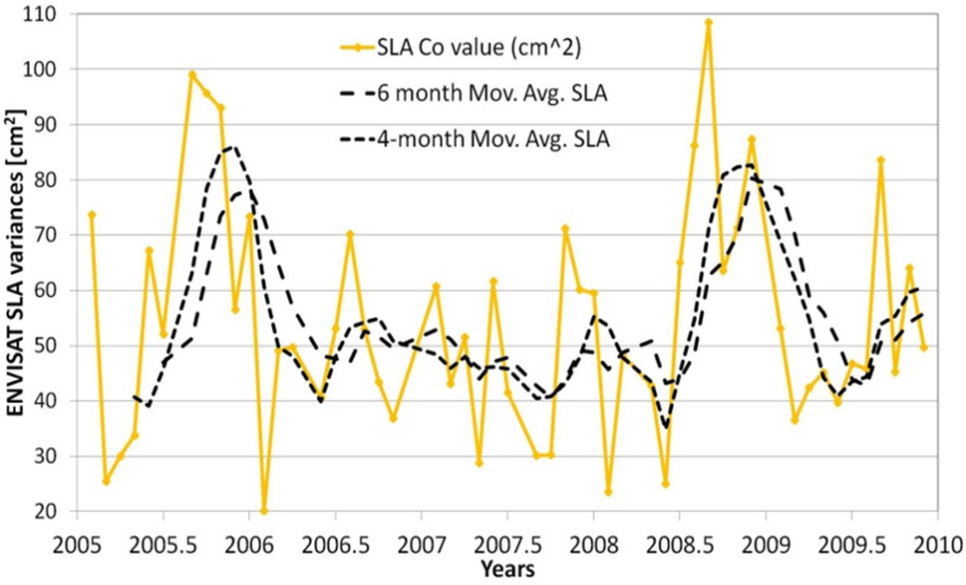

Figure 4: *ENVISAT SLA variance variability for the period under study.*

5. SLA ANALYTICAL COvariance functiosn and prediction with LSC

As already mentioned, empirical covariance functions have been determined for pass 444 for all available ENVISAT cycles. Following that, analytical covariance function models are determined and prediction with LSC is carried out in the along-track direction to test their performance. An analytical example is presented below, where the analysis for a single ENVISAT cycle (cycle 74) and pass 444 are given. The results presented below refer to a single month of the satellite data (August 2005) in order to depict the performance of the analytical models. All models will be denoted as MODEL A, B, …, F (exponential ones corresponding to Eqs. 5-10) MODEL G and H refers to 2nd and 3rd order Gauss-Markov ones while MODEL I refers to the last analytical model that is tested. In Figure 5, the empirical covariance function of the SLA is depicted with dotted line, along with the fitted analytical models (Models A, B, …I). From Figure 5, the exponential models seem to provide a good fit to the empirical values, as the Gauss-Markov models do. The only model that seems to miss-model the empirical one is the one based on Legendre polynomials (MODEL I), probably due to the limited number of observations and the limited extend of the area under study. The latter result in the difficulties in the estimation of the parameters needed for MODEL I (see Eq. 14) and unstable results. When the same model is tested in a basin-wide estimation, then these problems are eliminated. The empirical SLAs have a variance of 99 cm^2 and a correlation length of 95.8 km, while the exponential models have a variance between

83 cm^2 (for model D) and 105 cm^2 (for model A) and correlation lengths from 80 km to 125 km. The second and third order Gauss-Markov models have variances of 87.4 cm^2 and 95.1 cm^2 respectively with a characteristic distance to 126 km and 83 km. The aforementioned values resemble pretty well the statistical behaviour of the empirical ones, while MODEL I gives unrealistic results with a variance of 101 cm^2 and a correlation length of 284 km. The latter signals that the Legendre polynomial model does not manage to fit the empirical values, so its estimates with LSC should have large errors.

The same analysis to derive analytical covariance functions for the ENVISAT SLAs has been followed for the 2D cases, where two prediction scenarios have been followed. The first one refers to the use of the entire ENVISAT SLA dataset for the Mediterranean Sea, during which only half of the points are used for the prediction to the locations of those not used. In the second case, the entire ENISAT SLA dataset is used again, but with an inner window completely removed (bounded between $32^o \leq \varphi \leq 36^o$ and $15^o \leq \lambda \leq 20^o$) so that the prediction is carried out from the remaining dataset in this inner region. The first case resembles the scenario that abundant, well-distributed and homogeneous observations are available for the prediction with LSC, while the latter to the event that prediction needs to be carried out to a completely un-surveyed area which is surrounded by observations. As far as the 2D test case with the windowed area is concerned, six models have been examined; four exponential and the two Gauss-Markov models, i.e., the ones that provide the best fit for the 1D case. The exponential models fit to the empirical values while the two Gauss-Markov models miss-model the empirical one in the first part of the function (see Figure 6). This is also obvious in the prediction results which are presented in the sequel. The empirical SLAs have a variance of 57 cm^2 and a correlation length of 12.4 km, while the analytical models have a variance between43 cm^2 (for model G) and 58 cm^2 (for models F and G) and correlation lengths from 20 km to 35 km. Finally, the empirical and analytical covariance functions for the 2D case where the prediction is carried out every second observation point have been determined. Once again the exponential models provided the best fit with the Gauss-Markov ones giving problematic fits to the first part of the empirical covariances. This was especially evident for the third order model that provided a very small correlation length (61 km compared to 100 km for the empirical model), showing that it completely miss-represents the variability of the SLA.

After the determination of the empirical covariance functions and the fitting of analytical models to the empirical values, prediction is carried out with LSC method, in order to investigate the accuracy of each model. For pass 444 three tests are performed. The first one by omitting the first 20 records of the track and using the rest for the prediction (TEST A), the second by omitting the last 20 points (TEST B) and the third by omitting every second point (TEST C) using the rest for the pre-

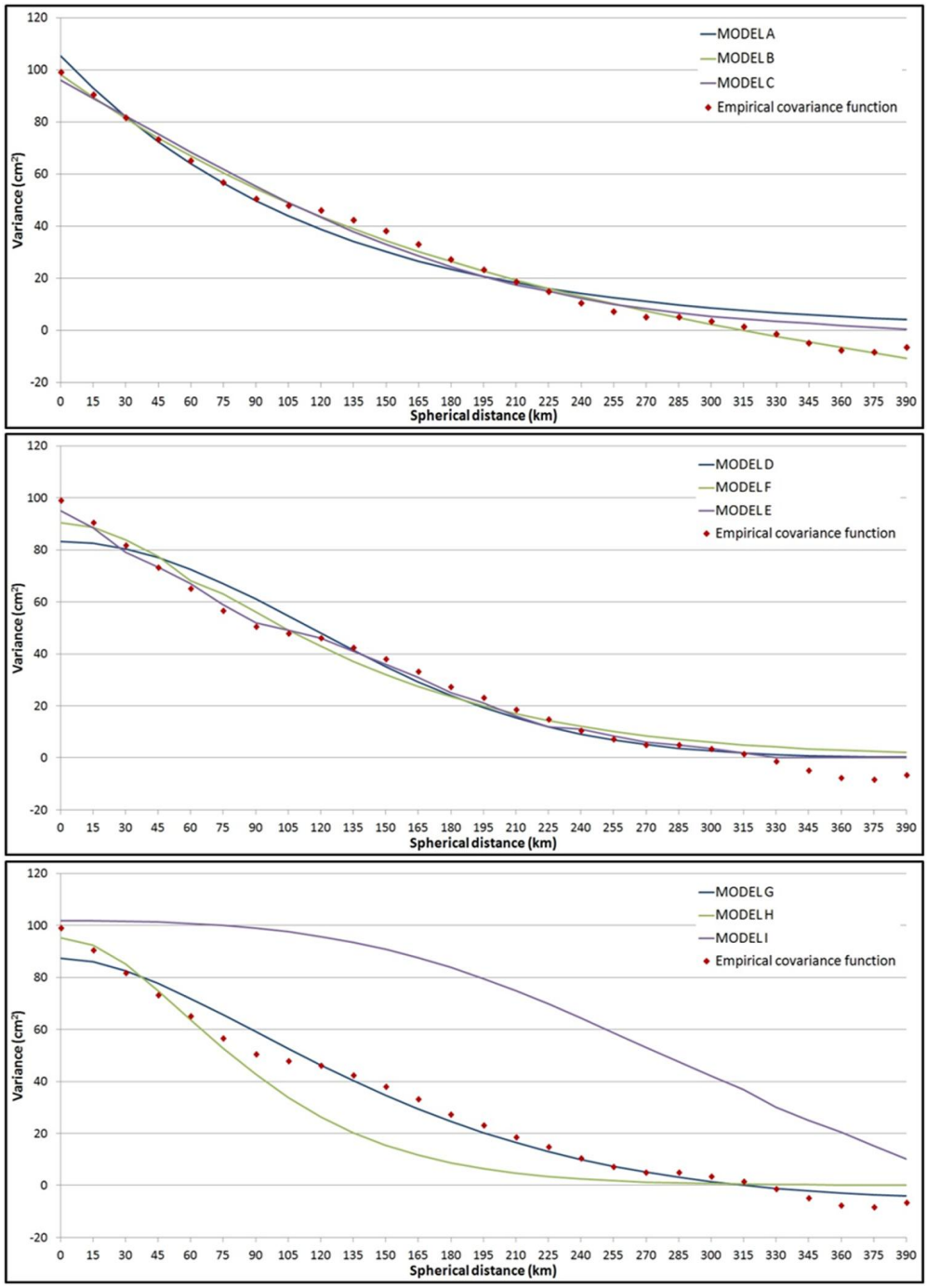

Figure 5: *ENVISAT SLA empirical and analytical covariance functions for pass 444.*

Table 2: *Statistics of the ENVISAT pass 444 SLAs and prediction errors from the various analytical models for all test cases investigated. Unit: [cm].*

SLA	min	max	mean	std
	-19.9	23.5	7.4	±8.5
TEST A				
MODEL A	-29.01	3.7	-10.1	±8.9
MODEL B	-18.6	5.1	-4.0	±6.1
MODEL C	-27.8	4.5	-8.5	±8.8
MODEL E	-27.7	4.5	-8.6	±8.7
MODEL F	-22.2	9.5	-0.8	±9.4
MODEL G	-18.9	11.5	1.7	±8.7
MODEL H	-20.8	22.5	7.3	±12.9
MODEL I	-91.3	-2.70	-35.7	±32.5
TEST B				
MODEL A	-13.39	5.95	-6.13	±5.54
MODEL B	-128.22	-10.89	-78.97	±35.41
MODEL C	-13.55	6.57	-5.99	±5.78
MODEL E	-13.74	6.38	-6.23	±5.78
MODEL F	-10.57	8.86	-3.15	±5.54
MODEL G	-10.19	10.42	-2.24	±5.94
MODEL H	-15.40	5.79	-7.73	±6.31
MODEL I	22.36	79.54	30.72	±28.59
TEST C				
MODEL A	-7.61	5.08	-0.11	±1.99
MODEL B	-7.57	5.10	-0.06	±1.88
MODEL C	-7.52	5.09	-0.10	±1.95
MODEL D	-86.59	17.39	-1.43	±12.47
MODEL E	-7.55	5.09	-0.10	±1.95
MODEL F	-8.98	5.27	-0.08	±2.07
MODEL G	-9.00	5.27	-0.07	±2.07
MODEL H	-9.94	5.29	-0.08	±2.18
MODEL I	-11.58	10.37	-0.08	±4.57

diction. The test cases are also depicted with related boxes in Figure 7, where the SLA for August 2005 and the sub-satellite points for pass 444 are displayed. Table 2 presents the statistics of the ENVISAT pass 444 for August 2005 and the prediction errors from the various analytical models for all three test cases. In TEST A, the exponential models B and E and the second order Gauss-Markov models give

the best results with the standard deviation (std) of the prediction errors at the ±6.1 cm and ±8.7 cm for the latter two. The difference of the 10 cm between the mean values of three models is positive in terms of the estimation of unbiased errors. The parameters estimated for model B were $a=105.20\ cm^2$, $b=-0.006$, $c=-7.001$ and $d=0.003$, for E $a=90.47cm^2$ and $b=0.015$, while for the 2nd order Gauss-Markov $\sigma^2_{h^{sla}} = 87.39\,\mathrm{cm}^2$ and D=115.32 km (see Eqs. 6, 9 and 11 respectively).

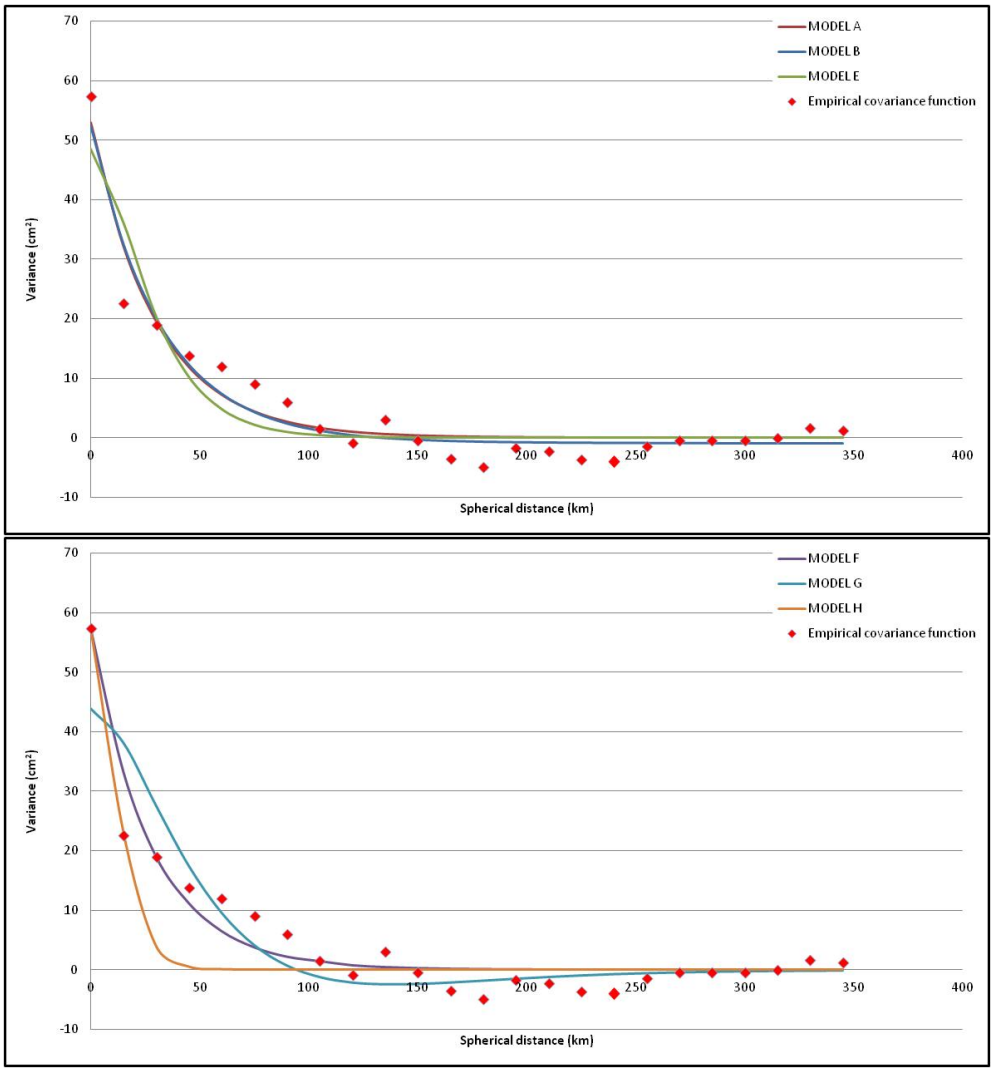

Figure 6: *Empirical and analytical SLA covariance functions (2D case for prediction in the windowed area).*

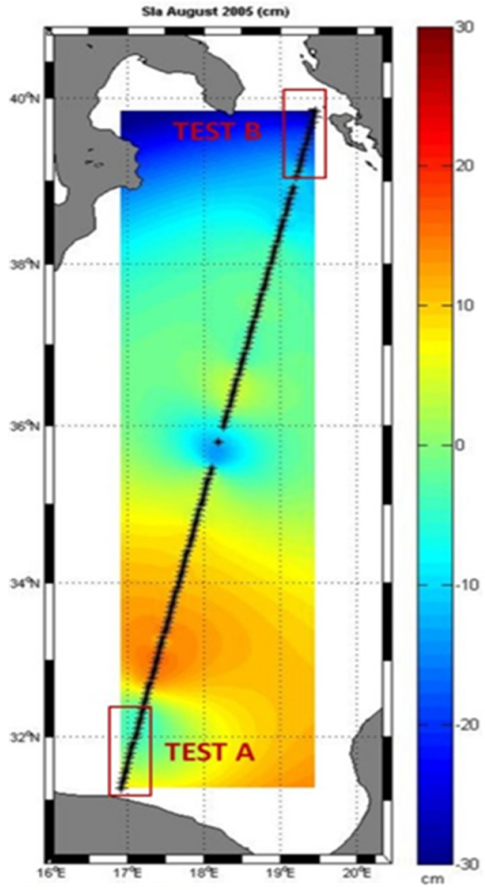

Figure 7: *ENVISAT SLAs along pass 444 and test areas.*

The prediction with model B has a std lower by ~30% compared to the data error, while the rest provide estimates with errors as large as that of the input signal. This is due to the fact that the first twenty points to be predicted have an SLA signal that cannot be modeled by the input data, probably because they are very close to dry-land and shallow water regions. The same behavior is presented in the results for TEST B, where the exponential models E and F and the second order Gauss-Markov model give the smallest prediction errors, with a std at the ±5.5-5.9 cm level. These std's are smaller by 35% compared to the error of the input data, which implies that even though prediction is carried out in an area where no information exists, the statistical characteristics of the used information is sufficient to provide more reliable (compared to TEST A) results. This difference can be due to the fact that TEST B is carried out in a region with large depths, so the SLA signal is not affected by land contamination and/or shallow-water backscatter effects. From these two tests, which simulate the case where SLA data from altimetry need to be predicted close to the coastline, the third order Gauss-Markov and that of the

expansion in Legendre polynomials present the largest errors. Almost all analytical models perform well in TEST C, giving small errors of few cm (±1.95-2.18 cm) and mean values at the sub-mm level. This is the case that sufficient information is available for the prediction to be carried out, so that the empirical and analytical covariance models describe more reliably and accurately the variability of the SLAs. The prediction errors are 77% smaller than the data input errors, which combined with the practically zero mean values allows the conclusion that the predictions are both reliable and unbiased. MODEL I does not perform well again, giving a standard error of ±4.5 cm.

For cycle 74 predictions were made by omitting every second point, using the rest to estimate the SLA in these locations (TEST D in the sequel) and the same prediction has been made for the inner window area bounded between $32^o \leq \varphi \leq 36^o$ and $15^o \leq \lambda \leq 20^o$ (TEST E). Table 3, summarizes the results for the prediction errors estimated in TEST D & TEST E for some of the analytical models that have been used in 1D case. From Table 3, it is obvious that exponential model E and that of the Gauss-Markov models provide again the best results, with a std at the ±3.6-4.5 cm level and with a mean value close to zero. The exponential model D is not reported in the results because it gave unrealistic prediction errors, which was due to the small variance determined (see also the previous section for the 1D case). The range of the Gauss- Markov models is much larger compared to that of the exponential models (~40 cm), signaling that in wider areas, planar analytical models

Table 3: *Statistics of prediction errors from the various analytical models for TEST D and TEST E. Unit: [cm].*

	min	**max**	**mean**	**std**
TEST D				
SLA	-50.90	55.40	7.33	±11.49
MODEL A	-34.88	29.31	-0.03	±3.65
MODEL B	-34.88	29.37	-0.03	±3.65
MODEL C	-34.88	29.36	-0.03	±3.65
MODEL E	-34.89	29.39	-0.03	±3.65
MODEL F	-47.95	55.15	-0.02	±4.57
MODEL G	-47.97	55.18	-0.02	±4.57
MODEL H	-80.37	89.49	-0.02	±5.77
TEST E				
SLA	-44.80	19.80	0.04	±7.50
MODEL A	-30.91	29.50	0.19	±7.40
MODEL E	-30.91	29.50	0.19	±7.39
MODEL G	-403.55	234.2	1.03	±34.63

cannot provide rigorous estimates. In TEST E, where an entire window within the study area is selected, all models give disappointing results, as the smallest std of the prediction errors is at the ±7.39 cm (MODEL E) when the std of the original field is ±7.50 cm. The rest of the exponential models (apart from MODEL D) are not reported since they provided similar results with MODEL A. The estimated prediction errors are not reliable due to the fact that the area where predictions are made is quite large ($4^o \times 5^o$) and contains no data, so that the rest of the observations cannot describe the SLA variability.

6. Conclusions

The use of satellite altimetry data from the exact repeat mission of ENVISAT to monitor SLA variations has been presented. The study referred to the detection of trends in the sea level for short time periods of one to three months, based on corrected altimetric SLA geophysical data records. The data analyzed referred to along-track records for one track that span the entire Aegean Sea in the north-south direction. In that case the trends determined from ENVISAT data are of the order of ~3-6 mm per 35-days to 3-motnhs and are in agreement with the 20-year long global trends identified from the analysis of all available altimetric records.

As far as the empirical covariance functions of ENVISAT SLA are concerned, it was noticed that there is a significant annual variation which is evident for the entire period under study. The annual SLA variations are in line with the thermal expansion of the sea, due to the increasing temperatures during the summer and early fall months and the lower temperatures during winter. This seasonal cycle can be also attributed to atmospheric forcing due to the variation in atmospheric pressure in the Mediterranean. Additionally, an analysis on the determination of analytical covariance functions for the SLA has been presented, using various models. The tests performed refer to both along-track (1D) and cross-track (2D) cases, where LSC method has been used to estimate the SLA either for prediction in areas close to the coastline or in a case where gaps are present. From all tests carried out, the exponential models (Model E) and the 2nd order Gauss-Markov one provided the best results in terms of prediction accuracy (std and mean of prediction errors), which were at the few cm level. In all cases, the parameters of the analytical covariance models have been determined so that they fit the empirical covariance values. The results acquired with the model based on the expansion in Legendre polynomials were disappointing, which is a subject that needs to be investigated further. Some key issues may relate to the scaling factor used, which is estimated within the fit to the empirical values as well as to the small number of data used. A point that is also a matter of future work is to include time as a variable in the employed analytical models, in order to attempt to model the variability of SLA over time with LSC.

Acknowledgement

The authors wish to acknowledge the funding provided for this work by the European Space Agency in the frame of the ESA-PRODEX GOCESeaComb project (C4000106380).

References

AVISO (2013) Available from www.aviso.oceanobs.com/msl. Accessed May 2013.

Barzaghi R., Tselfes N., Tziavos I.N., Vergos G.S., 2009. Geoid and High Resolution Sea Surface Topography Modelling in the Mediterranean from Gravimetry, Altimetry and GOCE Data: Evaluation by Simulation. *Journal of Geodesy*, **83(8)**, 751-772. doi: 10.1007/s00190-008-0292-z.

Bindoff N.L., Willebrand J., Artale V., Cazenave A., Gregory J., Gulev S., Hanawa K., Le Quéré C., Levitus S., Nojiri Y., Shum C.K., Talley L.D. and Unnikrishnan A., 2007. Observations: Oceanic Climate Change and Sea Level. In: Solomon S., Qin D., Manning M., Chen Z., Marquis M., Averyt K.B., Tignor M. and Miller H.L. (Eds.) *Climate Change 2007: The Physical Science Basis*. Cambridge University Press, Cambridge, United Kingdom and New York, NY, USA.

Chambers D. P., Wahr J., and Nerem R.S., 2004. Preliminary observations of global ocean mass variations with GRACE, *Geophys. Res. Lett*., **31, L13310**, doi: 10.1029/2004GL020461.

Chen J. L, Wilson C.R., Tapley B.D., Famiglietti J.S., 2005. Seasonal global mean sea level change from satellite altimeter GRACE and geophysical models. *J Geod* **79**: 532-539,doi:10.1007/500190-005-005-9.

Garci D., Ramillien G., Lombard A. and Cazenave A., 2007. Steric sea-level variations inferred from combined Topex/Poseidon altimetry and GRACE gradiometry. *Pure Appl. Geophys.* **164**: 721-731.

Jordan S.K.,1972. Self-Consistent Statistical Models for the Gravity Anomaly, Vertical Deflections, and Undulation of the Geoid. *J. Geophys. Res.*, **77(20),** 3660-3670.

Knudsen, P., 1987. Estimation and modelling of the local empirical covariance function using gravity and satellite altimeter data. *Bull. Geod.* 61:45-160.

Knudsen P., 1993. Integration of gravity and altimeter data by optimal estimation techniques. In Lecture Notes in Earth Sciences "Satellite Altimetry for Geodesy and Oceanography" (Eds. R. Rummel and F. Sansò), *Springer-Verlag, Berlin Heidelberg*, **50**, 453-466

Knudsen P. and Tscherning C.C., 2007. Error Characteristics of dynamic topography models derived from altimetry and GOCE Gravimetry. In IAG Symposia "Dynamic Planet 2005 - Monitoring and Understanding a Dynamic Planet with Geodetic and Oceanographic Tools" (Eds. Tregoning P. and Rizos, C.), **Vol.130**. *Springer Berlin Heidelberg*, 11-16.

Tscherning C.C. and Rapp R.H., 1974. Closed covariance expressions for gravity anomalies, geoid undulations, and deflections of the vertical implied by anomaly degree-variance models. Reports of the Department of Geodetic Science, 208, The Ohio State University, Columbus, Ohio.

Tziavos I.N., Vergos G.S., Mertikas S.P., Daskalakis A., Grigoriadis V.N. and Tripolitsiotis A., 2013. The contribution of local gravimetric geoid models to the calibration of satellite altimetry data and an outlook of the latest GOCE GGM performance in GAVDOS. *Adv. Space Res.*, **51(8)**, 1502-1522, doi: 10.1016/j.asr.2012.06.013.

Vergos G.S., Tziavos I.N. and Sideris M.G., 2012. On the determination of sea level changes by combining altimetric, tide gauge, satellite gravity and atmospheric observations. In: Kenyon S., Pacino C., Marti U. (Eds.) *Geodesy for Planet Earth*, IAG Symposia Vol. **136**, Springer Berlin Heidelberg New York, 123-130.

Vergos G.S., Natsiopoulos D.A. and Tziavos I.N., 2013. Sea level anomaly and dynamic ocean topography analytical covariance functions in the Mediterranean Sea from ENVISAT data. Proceedings of the European Space Agency "20 Years of progress in radar altimetry", ESA Publications SP-710.